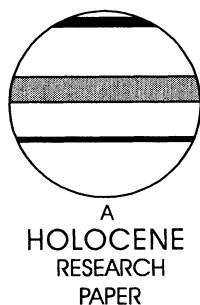


Winter and summer climate patterns in the European-Middle East during recent centuries as documented in a northern Red Sea coral record

Norel Rimbu,^{1*} Thomas Felis,² Gerrit Lohmann¹ and Jürgen Pätzold²

(¹Alfred-Wegener-Institute for Polar and Marine Research, 27570 Bremerhaven, Germany; ²DFG-Research Center for Ocean Margins, University of Bremen, 28359 Bremen, Germany)

Received 23 August 2004; revised manuscript accepted 8 November 2005



Abstract: The Ras Umm Sidd coral $\delta^{18}\text{O}$ record from the northern Red Sea is the northernmost centuries-long coral time series that is currently available in seasonal resolution (AD 1750–1995). Here we investigate climate patterns associated with the coral $\delta^{18}\text{O}$ time series separately for boreal winter and summer, using instrumental and reconstructed climate fields for the European-Middle East region. The winter coral $\delta^{18}\text{O}$ record is associated with dominant modes of sea-level pressure, temperature and precipitation variability in the European-Middle East region, which reflect the Arctic Oscillation/North Atlantic Oscillation (AO/NAO) phenomenon. The summer coral $\delta^{18}\text{O}$ record is associated with an atmospheric pattern having its main centre of action over southwestern Scandinavia/northern Great Britain. The connection between these large-scale atmospheric circulation patterns and the coral time series was stable during the past 250 years. During winter, eastern Mediterranean/Middle East climate, as reflected in the coral $\delta^{18}\text{O}$ record, is strongly controlled by the AO/NAO. In contrast, large-scale atmospheric circulation processes over the European-Middle East region are relatively less important for northern Red Sea climate during summer. The results suggest a high potential for seasonally resolved proxy records derived from fossil corals of the northern Red Sea to provide information on winter and summer climate patterns of the Middle East-European region for time intervals of the Holocene epoch or the last interglacial period.

Key words: Coral, oxygen isotopes, climate variability, seasonal climate, Red Sea, Middle East, Arctic Oscillation, North Atlantic Oscillation, atmospheric circulation.

Introduction

The northern Red Sea is an exceptionally northern site of coral reef growth, located at a latitude of 28–29° N. In the context of understanding the natural climate variability of the eastern Mediterranean/Middle East region and Europe during the past, proxy records derived from annually banded reef corals of the northern Red Sea play an important role (Felis *et al.*, 2000; Rimbu *et al.*, 2001, 2003; Felis *et al.*, 2004). This narrow, desert-surrounded ocean basin is strongly influenced by mid-latitude continental climate (Rimbu *et al.*, 2001, 2003), and is very sensitive to atmospheric processes owing to a relatively weak stratification of the water column (Felis *et al.*, 1998; Eshel *et al.*, 2000). Subsequent studies have noted the potential

of northern Red Sea corals for documenting climate variability over the Mediterranean basin and the European-Atlantic sector (Pauling *et al.*, 2003; Paz *et al.*, 2003; Greatbatch *et al.*, 2004; Tourre and Paz, 2004; Hall *et al.*, 2005; Kondrashov *et al.*, 2005; Luterbacher *et al.*, 2006).

Massive, annually banded corals from the surface waters of the tropical and subtropical oceans provide a seasonally resolved archive of past climate variability. Isotopic and elemental tracers, incorporated into the carbonate skeletons of these corals during growth, provide proxies of past environmental variability of the surface ocean (eg, Felis and Pätzold, 2004). A coral record from Ras Umm Sidd near the southern tip of the Sinai Peninsula (northern Red Sea) is the northernmost centuries-long coral time series that is currently available in seasonal resolution, covering the period AD 1750–1995 (Felis *et al.*, 2000). This time series is based on

*Author for correspondence (e-mail: nrumbu@awi-bremerhaven.de)

measurements of oxygen isotopes ($\delta^{18}\text{O}$) in the skeleton of a single coral colony (*Porites* sp.). Coral $\delta^{18}\text{O}$ provides a proxy for the temperature and the $\delta^{18}\text{O}$ of the ambient seawater at the time of coral growth, with the latter being related to the hydrologic balance. Coral $\delta^{18}\text{O}$ is inversely related to temperature and positively related to salinity variations.

The Ras Umm Sidd coral $\delta^{18}\text{O}$ record was shown to reflect variations in regional sea-surface temperature (SST) and aridity on interannual and longer timescales, with varying proportions of these two environmental parameters through time (Felis *et al.*, 2000). Because coral $\delta^{18}\text{O}$ integrates variations in temperature and hydrologic balance, the record may better represent atmospheric circulation changes throughout the eastern Mediterranean/Middle East region than proxy records that reflect a single climate variable. Significant correlations between annually averaged coral $\delta^{18}\text{O}$ and northern Red Sea gridded SST as well as southeastern Mediterranean station-based temperature, precipitation and sea level pressure were reported (Felis *et al.*, 2000). It was shown that the interannual to decadal variability in the Ras Umm Sidd coral $\delta^{18}\text{O}$ record is strongly linked to large-scale atmospheric climate phenomena such as the North Atlantic Oscillation (NAO) (Felis *et al.*, 2000) and the Arctic Oscillation (AO) (Rimbu *et al.*, 2001), consistent with the strong influence of these phenomena on the eastern Mediterranean/Middle East region (Paz *et al.*, 2003; Tourre and Paz, 2004).

In this study we test whether the spatial patterns of large-scale atmospheric circulation and SST associated with Ras Umm Sidd coral $\delta^{18}\text{O}$ variability as described in previous studies (eg. Rimbu *et al.*, 2001, 2004) are consistent with coral-based patterns in the fields of temperature and precipitation over land. Furthermore, we test if the spatial climate patterns associated with coral $\delta^{18}\text{O}$ variability are stable over longer periods, by extending the analyses into the pre-instrumental period. We focus on the two seasonal extremes in the Ras Umm Sidd coral record, by separately investigating the coral $\delta^{18}\text{O}$ time series of boreal winter and summer. Recent work has shown that fossil corals from the northern Red Sea provide a great potential for seasonally resolved climate reconstructions during time intervals of the Holocene epoch and the last interglacial period (Felis *et al.*, 2003, 2004). Our detailed analyses of $\delta^{18}\text{O}$ variability in the modern coral record from Ras Umm Sidd and its relation to dominant modes of sea-level pressure (SLP), temperature and precipitation variability in the European-Middle East region (hereafter EME region) will improve the climatic interpretation of proxy records derived from fossil corals of the northern Red Sea.

The paper is organized as follows. Data and methods are described in the next section. In the following section we discuss the spatial patterns of atmospheric circulation, temperature and precipitation associated with coral $\delta^{18}\text{O}$ variability during boreal winter. We then go on to investigate the variability of the coral $\delta^{18}\text{O}$ record during boreal summer and its associated spatial climate patterns. The asymmetry between the spatial patterns of atmospheric circulation associated with extreme positive and extreme negative values in both the winter and summer coral $\delta^{18}\text{O}$ records is then discussed. A discussion of the results and the main conclusions follow in the final two sections.

Data and methods

The Ras Umm Sidd coral $\delta^{18}\text{O}$ record from the northern Red Sea published by Felis *et al.* (2000) was generated from a living *Porites* sp. coral drilled in November 1995 near the southern

tip of the Sinai Peninsula (27° 50.9' N, 34° 18.6' E). The coral time series has a bimonthly resolution and covers the period AD 1750–1995. Six equally spaced values per year were derived from linear interpolation of the original coral $\delta^{18}\text{O}$ data of more than six samples per year. The non-cumulative, intra-annual age model error of the time series is in the order of 2–3 months. The cumulative, inter-annual age model error is less than 3 years at the bottom of the core (Felis *et al.*, 2000). In this study we analyse the winter (January–February, JF) and summer (July–August, JA) coral $\delta^{18}\text{O}$ records derived from the bimonthly time series, covering the common period of 1751–1995.

SLP data were extracted from an updated version of the historical SLP data set constructed by Trenberth and Paolino (1980). This data set is based on a combination of station-based SLP observations covering the period 1899 to present. The spatial resolution of this dataset is 5° latitude × 5° longitude.

Temperature and precipitation data over land are based on a recently published high-resolution (0.5° latitude × 0.5° longitude) data set developed at the Climate Research Unit (University of East Anglia) covering the period 1901–2002 (Mitchell and Jones, 2005). This data set (CRU TS 2.1) is based on temperature and precipitation observations at meteorological stations, corrected for inhomogeneities in the station records.

For the pre-instrumental period, we used reconstructed SLP data covering the area 30°–70° N; 30° W–40° E (Luterbacher *et al.*, 2002). This SLP reconstruction is based on a combination of early instrumental station series and documentary proxy data from Eurasian sites. Under the assumption of stationarity in the statistical relationships, a transfer function derived over the 1901–1990 period was used to reconstruct SLP fields for the last 500 years over the eastern North Atlantic-European region (5° × 5° latitude by longitude grid).

The AO index used in this study is defined as the time coefficients associated with the first EOF of Northern Hemisphere (20° N–90° N) SLP for January–February during the period 1901–1995, based on the updated data set of Trenberth and Paolino (1980). The NAO indices used in this study are based on station data as defined by Jones *et al.* (1997) for January–February (NAO-CRU), Hurrell *et al.* (2003) for December–March (NAO-H), as well as an improved version of the Gibraltar/Reykjavik NAO index for January–February (NAO-V) (Vinther *et al.*, 2003a) for the periods 1824–1995, 1864–1995 and 1821–1995, respectively. In addition, we have used two annually resolved reconstructions of the winter NAO index based on tree-rings (Cook *et al.*, 2002) for the period 1751–1979 (extended by instrumental data to 1995) and based on $\delta^{18}\text{O}$ in Greenland ice cores (Vinther *et al.*, 2003b) for the period 1751–1970.

In this study, the spatial climate patterns associated with variability in the coral $\delta^{18}\text{O}$ time series are based on conventional linear correlation analysis (von Storch and Zwiers, 1999). The coral $\delta^{18}\text{O}$ time series was correlated with climate field anomalies from each grid point and the field of correlation coefficients, referred to as correlation map, was investigated to identify large-scale spatial patterns of significant correlations. The significance of the correlations was derived using *t*-test statistics (von Storch and Zwiers, 1999). In addition, the spatial climate patterns associated with variability in the coral $\delta^{18}\text{O}$ time series were compared with spatial patterns associated with dominant modes of SLP, temperature and precipitation variability over the EME region as derived from Empirical Orthogonal Function (EOF) analysis (von Storch and Zwiers, 1999).

Finally, the symmetry of the averaged SLP patterns associated with extreme positive (higher than $0.75 \times$ standard deviation) and extreme negative (lower than $-0.75 \times$ standard deviation) values of $\delta^{18}\text{O}$ in the coral time series were assessed. The threshold of $0.75 \times$ standard deviation was chosen as a compromise between the strength of a pattern and its number of realizations.

Winter coral $\delta^{18}\text{O}$ variability and associated climate patterns

The Ras Umm Sidd winter coral $\delta^{18}\text{O}$ record shows a negative linear trend towards the present. This trend could reflect a tendency towards warmer/less arid winter conditions in the northern Red Sea since the mid-eighteenth century. Because the climatic interpretation of long-term trends in coral $\delta^{18}\text{O}$ records is problematic (eg, Felis and Pätzold, 2004), the linear trend was removed from the coral record prior to statistical analyses. The detrended winter coral $\delta^{18}\text{O}$ time series reveals pronounced interannual and decadal variations (Figure 1). High (low) values in coral $\delta^{18}\text{O}$ reflect colder/more arid (warmer/less arid) conditions in the northern Red Sea region (Felis *et al.*, 2000). Such conditions are associated with various regional and global atmospheric circulation patterns (Felis *et al.*, 2000; Eshel *et al.*, 2000; Rimbu *et al.*, 2001, 2003, 2004; Paz *et al.*, 2003; Felis *et al.*, 2004; Tourre *et al.*, 2004).

The correlation map for the winter coral $\delta^{18}\text{O}$ record and winter SLP fields over the EME region during the period 1901–1995 shows significant positive correlations (95% confidence level) over the Mediterranean basin, and significant negative correlations over northern Europe (Figure 2a). This spatial pattern strongly resembles that of the dominant mode of winter SLP variability (EOF1) in this region during the corresponding period (Figure 2d). The correlation coefficient between the winter coral $\delta^{18}\text{O}$ record and the time coefficients associated with the first EOF of winter SLP variability in

the EME region is $+0.33$, which is slightly higher than the correlation of coral $\delta^{18}\text{O}$ and the NAO-CRU index ($r = +0.30$) during the corresponding period. The winter coral $\delta^{18}\text{O}$ record is best correlated with the AO index ($r = +0.35$), consistent with the strong influence of the AO on the climate of the eastern Mediterranean/Middle East (Rimbu *et al.*, 2001; Felis *et al.*, 2004; Tourre and Paz, 2004). Furthermore, the time coefficients associated with the first EOF of winter SLP in the EME region are correlated slightly higher with the AO index ($r = +0.82$) than with the NAO-CRU index ($r = +0.78$).

The winter coral $\delta^{18}\text{O}$ record is significantly negative correlated with winter temperature over land in the southern and eastern Mediterranean region during the period 1901–1995 (Figure 2b). The highest negative correlations occur over the Sinai Peninsula and northern Arabia, consistent with the site of coral collection near the southern tip of the Sinai Peninsula as well as with the inverse relationship between coral $\delta^{18}\text{O}$ and temperature. Significant positive correlations occur over northern Europe. This spatial pattern strongly resembles that of the dominant mode of winter temperature variability (EOF1) in the EME region during the corresponding period (Figure 2e). The correlation between the winter coral $\delta^{18}\text{O}$ record and the time coefficients associated with the first EOF of winter temperature variability in the EME region is $+0.40$. EOF1 of EME winter temperature variability is also significantly correlated with the NAO-CRU index ($r = +0.86$) and the AO index ($r = +0.79$).

The correlation map for the winter coral $\delta^{18}\text{O}$ record and winter precipitation over land shows an alternating spatial pattern with positive correlations over northern Europe, negative correlations over southern Europe and positive correlations south of the Mediterranean Sea during the period 1901–1995 (Figure 2c). However, areas of significant correlations only occur over central/southwestern Scandinavia, Scotland, western France, Iberia, Italy, the Balkans, southwestern Turkey and Algeria/Tunisia/Libya. No significant correlation occurs with local precipitation, owing to the negligible

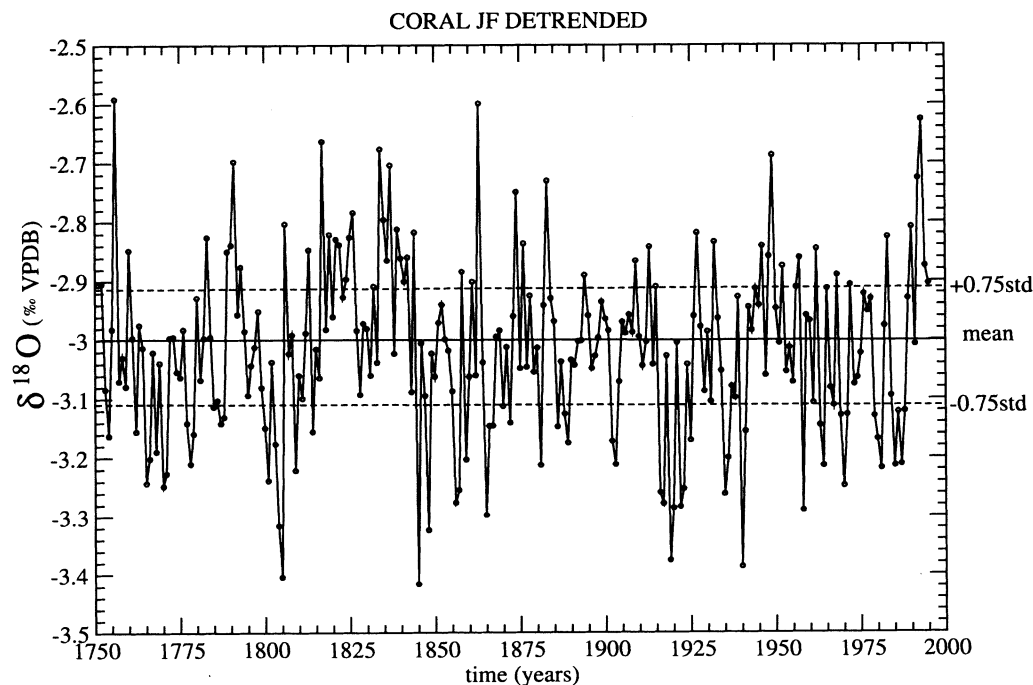


Figure 1 The winter coral $\delta^{18}\text{O}$ time series of the bimonthly resolved Ras Umm Sidd coral record from the northern Red Sea published by Felis *et al.* (2000). The linearly detrended time series for January–February (JF) is shown (AD 1751–1995). Dashed lines represent $+0.75/-0.75$ standard deviations. High (low) values in coral $\delta^{18}\text{O}$ reflect colder/more arid (warmer/less arid) conditions in the northern Red Sea (Felis *et al.*, 2000)

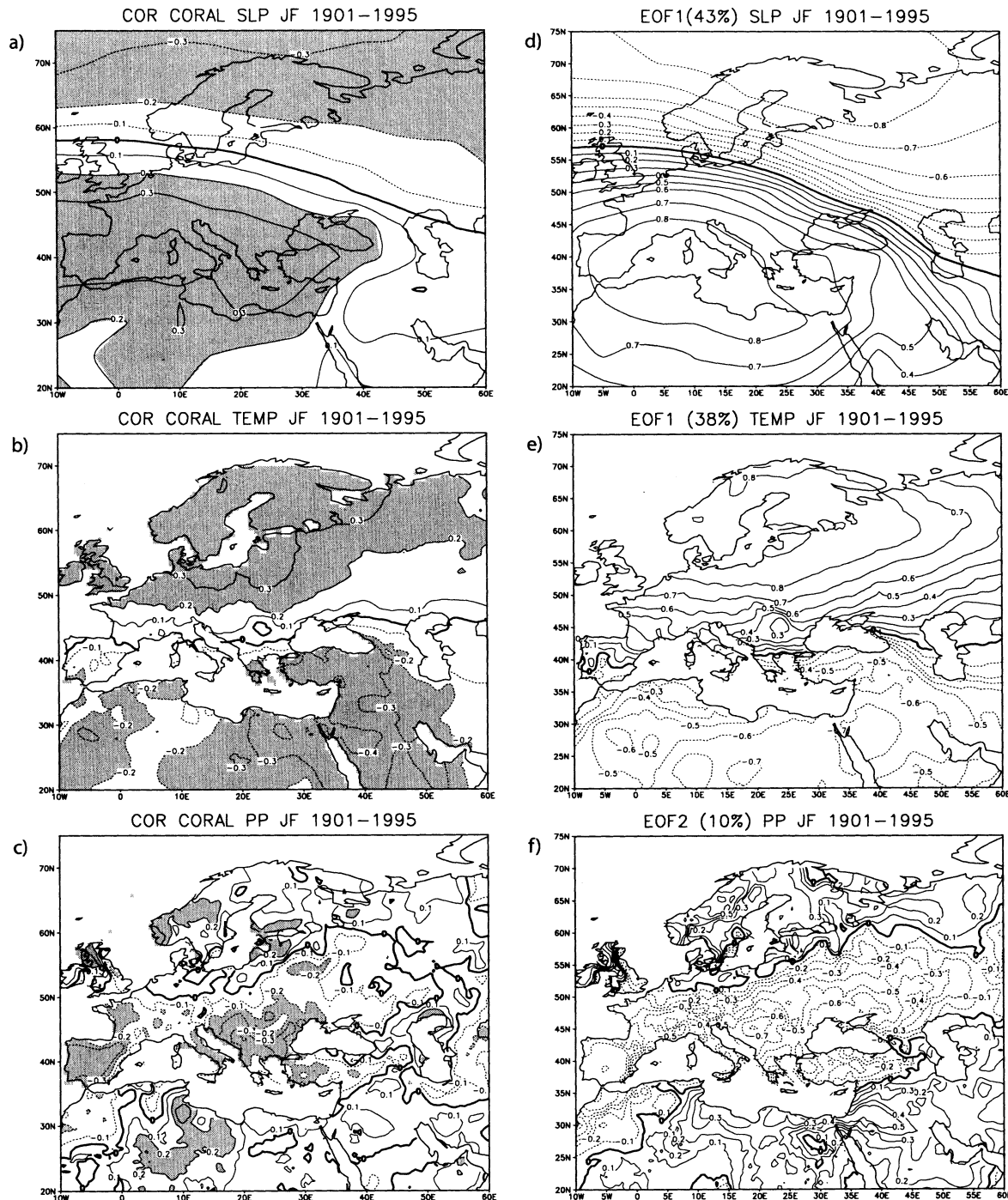


Figure 2 The correlation maps for the winter coral $\delta^{18}\text{O}$ record and fields of (a) sea-level pressure (SLP), (b) temperature and (c) precipitation over the European-Middle East (EME) region for January–February (JF) are shown. Shaded areas indicate correlations significant at the 95% confidence level. The corresponding first Empirical Orthogonal Functions (EOFs) of (d) SLP and (e) temperature, and (f) the second EOF of precipitation over the EME region for JF are also shown. The variance explained by each EOF is indicated. Prior to the analyses the data were detrended and normalized. The period is AD 1901–1995. SLP data are from Trenberth and Paolino (1980), temperature and precipitation data over land are from Mitchell and Jones (2005)

amounts of winter precipitation in the arid northern Red Sea region (Felis *et al.*, 2000). The spatial pattern resembles that of the second EOF of winter precipitation variability in the EME region during the corresponding period (Figure 2f). The correlation between the winter coral $\delta^{18}\text{O}$ record and the time coefficients associated with the second EOF of winter precipitation variability in the EME region is +0.35. EOF2 of EME winter precipitation variability is significantly correlated both with the NAO-CRU index ($r = +0.69$) and the AO index ($r = +0.67$). The first EOF of EME winter precipitation variability shows pronounced anomalies over northeastern

Europe and south of the Caspian Sea (Figure 3). The time coefficients associated with EOF1 are not significantly correlated with the winter coral $\delta^{18}\text{O}$ record ($r = +0.09$).

The spatial SLP, temperature and precipitation anomaly patterns associated with the winter coral $\delta^{18}\text{O}$ record are physically consistent. Positive (negative) SLP anomalies over the Mediterranean basin are associated with advection of colder (warmer) air from southeastern Europe (northeastern Africa) to the northern Red Sea region, inducing negative (positive) SST anomalies. The negative (positive) SST anomalies are recorded as positive (negative) $\delta^{18}\text{O}$ anomalies in the

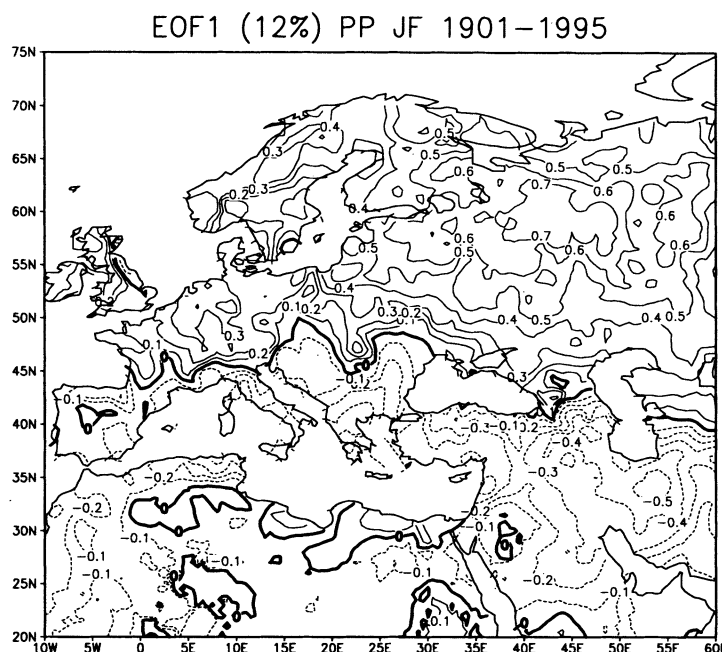


Figure 3 The first Empirical Orthogonal Function (EOF) of precipitation over the European-Middle East region for January–February (JF) is shown. The variance explained by the EOF is indicated. Prior to the analysis the data were detrended and normalized. The period is AD 1901–1995. Precipitation data over land are from Mitchell and Jones (2005)

coral skeleton (Felis *et al.*, 2000). Through this physical mechanism, the coral $\delta^{18}\text{O}$ record is connected to the dominant modes of SLP, temperature and precipitation variability of the EME region during winter. These modes are related to large-scale atmospheric phenomena such as NAO and AO, as suggested in previous studies (Felis *et al.*, 2000; Rimbu *et al.*, 2001).

In order to evaluate the stability of the large-scale atmospheric circulation pattern associated with winter coral $\delta^{18}\text{O}$ variability beyond the instrumental period we constructed a correlation map for the period 1751–1995, using reconstructed SLP fields for the region 10°W – 40°E ; 30°N – 70°N (Figure 4a). The spatial pattern strongly resembles the corresponding correlation pattern based on instrumental data (Figure 2a) as well as the spatial pattern associated with the first EOF of winter SLP variability during the period 1751–1995 (Figure 4b). The correlation between the winter coral $\delta^{18}\text{O}$ record and the time coefficients associated with the first EOF of winter SLP variability during 1751–1995 is +0.35. This demonstrates that the connection between the winter coral $\delta^{18}\text{O}$ record and the dominant mode of winter atmospheric circulation variability over the EME region was stable during the entire 1751–1995 period.

To better assess the stability of the connection between winter climate in the eastern Mediterranean/Middle East region, as reflected by the coral record, and the North Atlantic-European realm we present correlation coefficients between winter coral $\delta^{18}\text{O}$ and various long time series of NAO indices. The winter coral $\delta^{18}\text{O}$ record is significantly correlated with the NAO-CRU index (Jones *et al.*, 1997) ($r = +0.29$) for the period 1824–1995, the NAO-H index (Hurrell *et al.*, 2003) ($r = +0.35$) for the period 1864–1995, and the NAO-V index (Vinther *et al.*, 2003a) ($r = +0.29$) for the period 1821–1995. The winter coral $\delta^{18}\text{O}$ record is also significantly correlated with a tree-ring NAO index reconstruction (Cook *et al.*, 2002) ($r = +0.17$) for the period 1751–1995 and an ice core $\delta^{18}\text{O}$ NAO-index reconstruction (Vinther *et al.*, 2003b) ($r = +0.25$) for the period 1751–1970.

Summer coral $\delta^{18}\text{O}$ variability and associated climate patterns

Similar to the winter coral time series, a negative linear trend towards the present evident in the Ras Umm Sidd summer coral $\delta^{18}\text{O}$ record was removed prior to statistical analyses (see also the section above: ‘Winter coral $\delta^{18}\text{O}$ variability and associated climate patterns’). The detrended summer coral $\delta^{18}\text{O}$ time series reveals pronounced interannual and decadal variations (Figure 5).

The correlation map for the summer coral $\delta^{18}\text{O}$ record and summer SLP fields over the EME region during the period 1901–1995 shows significant positive correlations (95% confidence level) over southwestern Scandinavia and northern Great Britain (Figure 6a). In the eastern Mediterranean-Black Sea/Caspian Sea region the correlation reveals a dipolar spatial pattern that is consistent with an advection of relatively cold air to the northern Red Sea. The correlation map for the summer coral $\delta^{18}\text{O}$ record and summer temperature over land during the period 1901–1995 shows significant negative correlations along the western margin of the northern Red Sea and large parts of northeastern Africa (Figure 6b), consistent with the site of coral collection near the southern tip of the Sinai Peninsula as well as with the inverse relationship between coral $\delta^{18}\text{O}$ and temperature. Positive but non-significant correlations with temperature occur north of 45°N . The correlation map for the summer coral $\delta^{18}\text{O}$ record and summer precipitation over land during the period 1901–1995 shows small-scale features over the EME region, possibly reflecting local phenomena such as convection or orographic waves (Figure 6c). No significant correlation occurs with local precipitation, consistent with the fact that it does not rain in the arid northern Red Sea region during summer (Felis *et al.*, 2000). Clearly, it is evident that large-scale atmospheric circulation processes are less important in explaining the coral $\delta^{18}\text{O}$ variability during summer compared with the winter season.

In order to evaluate the stability of the large-scale atmospheric circulation pattern associated with summer coral

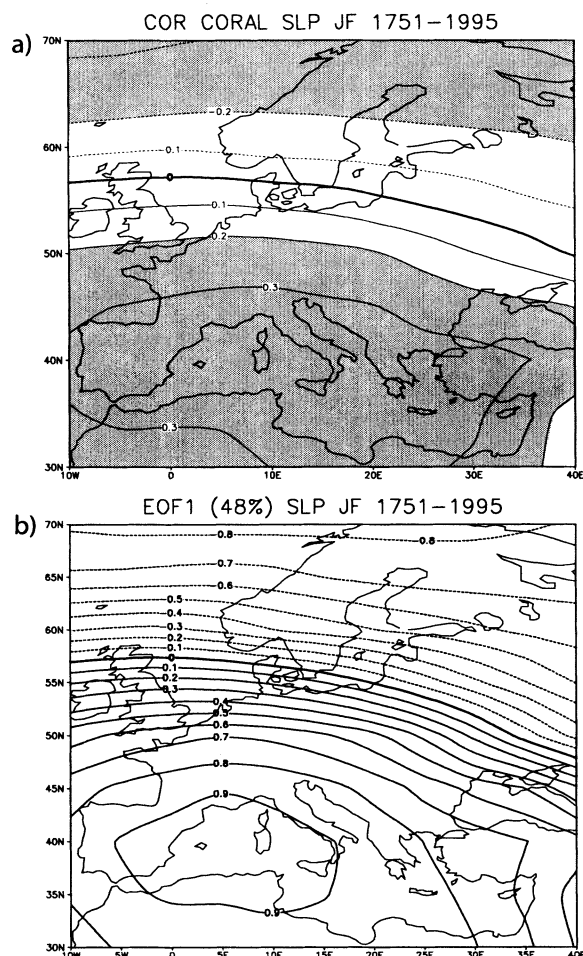


Figure 4 (a) The correlation map for the winter coral $\delta^{18}\text{O}$ record and reconstructed fields of sea-level pressure (SLP) over the European-Middle East (EME) region for January–February (JF) is shown. Shaded areas indicate correlations significant at the 95% confidence level. (b) The corresponding first Empirical Orthogonal Function (EOF) of reconstructed SLP over the EME region for JF is also shown. The variance explained by the EOF is indicated. Prior to the analyses the data were detrended and normalized. The period is AD 1751–1995. Reconstructed SLP data are from Luterbacher *et al.* (2002)

$\delta^{18}\text{O}$ variability beyond the instrumental period we constructed a correlation map for the period 1751–1995, using reconstructed SLP fields for the region 10°W – 40°E ; 30°N – 70°N (Figure 7a). The spatial pattern strongly resembles the corresponding correlation pattern based on instrumental data (Figure 6a), and has similarities to the spatial pattern associated with the second EOF of summer SLP variability during the period 1751–1995 (Figure 7b). The correlation between the summer coral $\delta^{18}\text{O}$ record and the time coefficients associated with the second EOF of summer SLP variability during 1751–1995 is +0.35. This demonstrates a stable connection between the summer coral $\delta^{18}\text{O}$ record and its associated spatial pattern of summer SLP variability over the EME region observed during the instrumental period (1901–1995) for the entire 1751–1995 period. This spatial pattern is also captured by the second EOF of summer SLP variability in this region during the corresponding period. The summer coral $\delta^{18}\text{O}$ record and the time coefficients associated with the first EOF of summer SLP variability (Figure 8) are not significantly correlated during the 1751–1995 period ($r = +0.07$).

In contrast to the winter season, EOF analyses of instrumental temperature and precipitation variability over

the EME region during summer do not reveal any dominant, stable EOFs. However, for SLP the spatial patterns associated with the first and second EOF of summer variability during the instrumental period (not shown) are very similar to those associated with the corresponding EOF1 and EOF2 for the entire 1751–1995 period (Figure 7b, 8), but their associated time coefficients are not significantly correlated with the summer coral $\delta^{18}\text{O}$ record during 1901–1995.

Asymmetry of associated climate patterns

In the previous sections we investigated the spatial climate patterns associated with Ras Umm Sidd coral $\delta^{18}\text{O}$ variability during winter and summer using linear methods. Here we apply composite analysis, which is a non-linear operation, in order to investigate the asymmetry of the atmospheric circulation patterns associated with the coral record during these two seasons.

The SLP anomaly patterns associated with extreme positive (Figure 9a) and extreme negative (Figure 9b) winter coral $\delta^{18}\text{O}$ anomalies are consistent with the physical mechanism that connects large-scale atmospheric circulation and the coral record from the northern Red Sea, as described in the section 'Winter coral $\delta^{18}\text{O}$ variability and associated climate patterns'. Extreme positive (negative) anomalies in the winter coral $\delta^{18}\text{O}$ record are associated with enhanced advection of colder (warmer) air from southeastern Europe (northeastern Africa) to the northern Red Sea. However, the two spatial patterns show some degree of asymmetry. The pattern associated with extreme positive winter coral $\delta^{18}\text{O}$ anomalies (Figure 9a) shows two centres of action, one over northeastern Europe and one over southwestern Europe. In contrast, the spatial pattern associated with extreme negative winter coral $\delta^{18}\text{O}$ anomalies (Figure 9b) shows a more zonal extension, especially over northern Europe. A simple visual inspection of the SLP anomaly maps averaged in the composite analysis reveals that 8 (10) out of 15 (26) SLP maps associated with extreme positive (negative) winter coral $\delta^{18}\text{O}$ anomalies are similar to the maps represented in Figure 9a (9b). Based on this simple approach, the spatial climate pattern associated with extreme positive winter coral $\delta^{18}\text{O}$ anomalies seems to be more robust than the pattern associated with extreme negative winter coral $\delta^{18}\text{O}$ anomalies. However, more rigorous significance tests are necessary in order to obtain a quantitative measure of the robustness of the atmospheric circulation patterns associated with positive/negative extremes in the winter coral $\delta^{18}\text{O}$ record.

Similar to the winter season, the SLP anomaly patterns associated with extreme positive (Figure 9c) and extreme negative (Figure 9d) summer coral $\delta^{18}\text{O}$ anomalies show some degree of asymmetry. Visual inspection of the SLP anomaly maps averaged in the composite analysis (19 for extreme positive and 17 for extreme negative summer coral $\delta^{18}\text{O}$ anomalies) reveals a high degree of variability. Only a small number of maps resemble the patterns represented in Figures 9c and 9d. This suggests that large-scale atmospheric circulation is less important in explaining the coral $\delta^{18}\text{O}$ variability during summer compared with the winter season, consistent with the results presented in the section 'Summer coral $\delta^{18}\text{O}$ variability and associated climate patterns'.

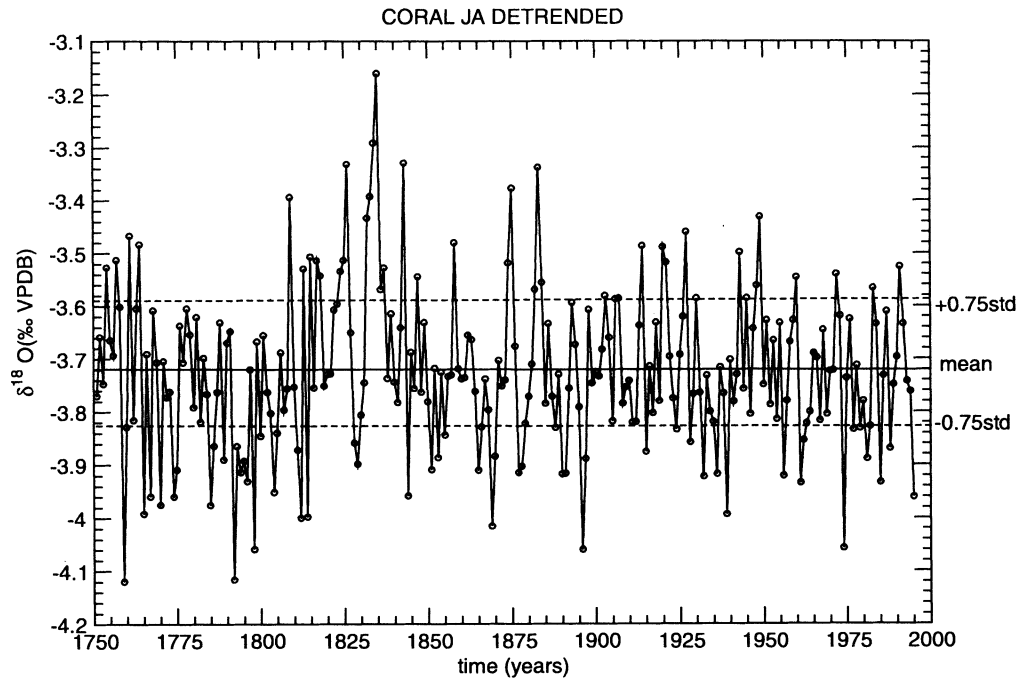


Figure 5 The summer coral $\delta^{18}\text{O}$ time series of the bimonthly resolved Ras Umm Sidd coral record from the northern Red Sea published by Felis *et al.* (2000). The linearly detrended time series for July–August (JA) is shown (AD 1751–1995). Dashed lines represent $+0.75/ -0.75$ standard deviations. High (low) values in coral $\delta^{18}\text{O}$ reflect colder/more arid (warmer/less arid) conditions in the northern Red Sea (Felis *et al.*, 2000)

Discussion

We have shown that both the winter and the summer time series of the bimonthly resolved Ras Umm Sidd coral $\delta^{18}\text{O}$ record from the northern Red Sea published by Felis *et al.* (2000) provide information on regional climate variability over the eastern Mediterranean/Middle East region as well as on large-scale climate patterns over the European-Middle East region. The results are consistent with previous work on this coral record from the northern Red Sea (Felis *et al.*, 2000; Rimbu *et al.*, 2001, 2004).

The winter coral $\delta^{18}\text{O}$ record is associated with the dominant modes of SLP, temperature and precipitation variability during the instrumental period (1901–1995) in the EME region (Figure 2). These modes are representative of the AO/NAO phenomenon in the atmosphere, and its associated spatial signatures in the temperature and precipitation fields over the region during winter. By using reconstructed SLP fields for the pre-instrumental period, we could show that the connection between the winter coral $\delta^{18}\text{O}$ record and the AO/NAO was stable during the past nearly 250 years (1751–1995) (Figure 4). Correlations with AO/NAO indices as well as SLP fields suggest that eastern Mediterranean/Middle East winter climate, as reflected in the winter coral $\delta^{18}\text{O}$ record, is stronger linked to the AO compared with the NAO, consistent with earlier findings (Rimbu *et al.*, 2001).

On a regional scale, high and significant correlations occur between the winter coral $\delta^{18}\text{O}$ record and temperature over the Sinai Peninsula and northern Arabia during the period 1901–1995 (Figure 2b), consistent with significant correlations between coral $\delta^{18}\text{O}$ and gridded SST in the northern Red Sea reported earlier (Felis *et al.*, 2000; Rimbu *et al.*, 2004).

On a regional scale, positive but weak (non-significant) correlations occur between the winter coral $\delta^{18}\text{O}$ record and precipitation along the southeastern margin of the

Mediterranean Sea (Figure 2c). The sign of the correlation is not consistent with the generally inverse relationship between coral $\delta^{18}\text{O}$ and local precipitation. However, this observation is consistent with earlier findings that colder/more arid conditions in the northern Red Sea, which are documented as high coral $\delta^{18}\text{O}$ anomalies, are associated with increased precipitation at stations along the southeastern margin of the Mediterranean Sea (Felis *et al.*, 2000). During such conditions, which occur during the AO/NAO high-index state, the total amount of precipitation that reaches the northern Red Sea from the north is negligible (Felis *et al.*, 2000), and other processes such as enhanced evaporation in the northern Red Sea resulting from lower tropospheric subsidence play a role (Eshel *et al.*, 2000). Paradoxically, such conditions are associated with decreased precipitation in Turkey (Felis *et al.*, 2000). This spatial anomaly pattern is associated with the second EOF of winter precipitation in the EME region (Figure 2f).

During the instrumental period (1901–1995), the summer coral $\delta^{18}\text{O}$ record is associated with an atmospheric circulation pattern over the EME region that consists of a wave train, with the main centre of action located over southwestern Scandinavia and northern Great Britain (Figure 6a). By using reconstructed SLP fields for the pre-instrumental period, we could show that the connection between the summer coral $\delta^{18}\text{O}$ record and this atmospheric circulation pattern was stable during the past nearly 250 years (1751–1995) (Figure 7a). This spatial pattern has similarities to that associated with the second EOF of summer SLP variability in the EME region during the period 1751–1995 (Figure 7b). This finding is consistent with the work of Xoplaki *et al.* (2003) who showed that summer temperature variability in the Mediterranean region is related to wave trains emanating from the North Atlantic. It was shown that intrusions of cold air in upper atmospheric levels that derive from a jet stream meandering between high and low geopotential height anomalies of alternating sign, which extend from the southeast of Greenland to the Caspian Sea,

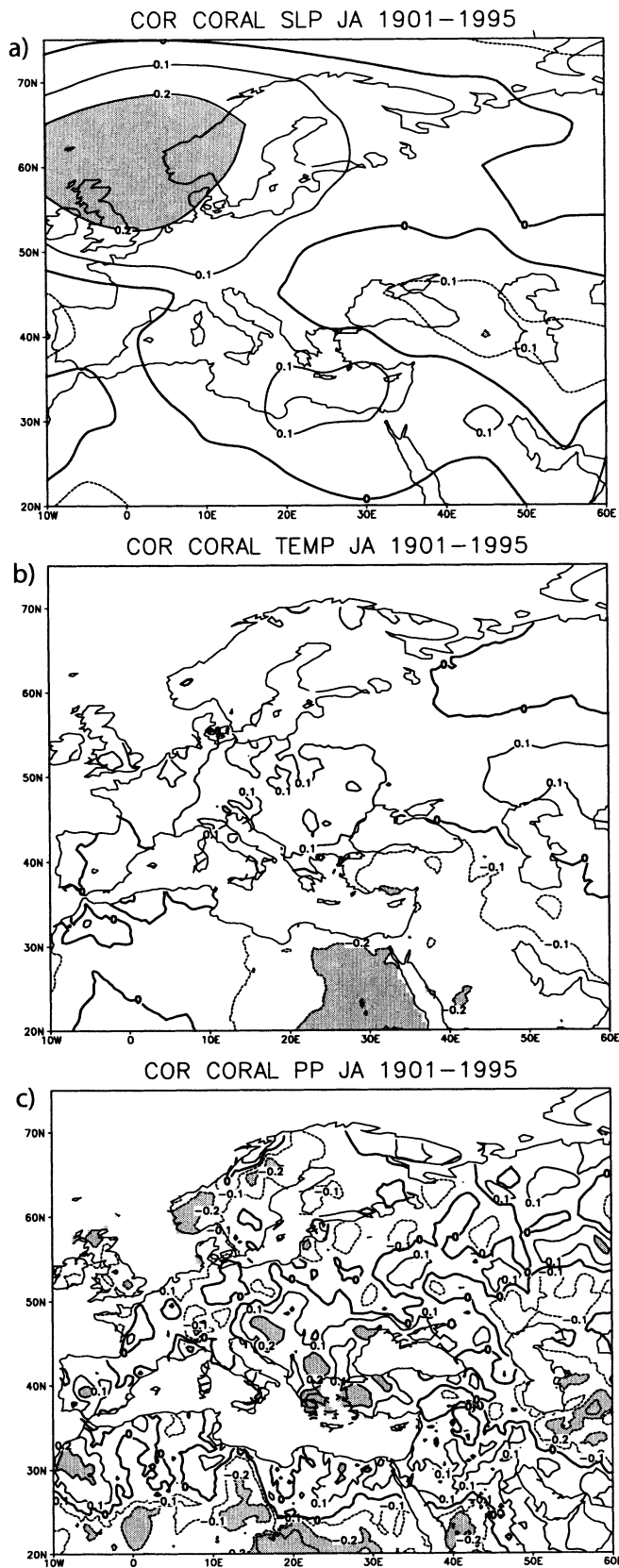


Figure 6 The correlation maps for the summer coral $\delta^{18}\text{O}$ record and fields of (a) sea-level pressure (SLP), (b) temperature and (c) precipitation over the European-Middle East (EME) region for July–August (JA) are shown. Shaded areas indicate correlations significant at the 95% confidence level. Prior to the analyses the data were detrended and normalized. The period is AD 1901–1995. SLP data are from Trenberth and Paolino (1980), temperature and precipitation data over land are from Mitchell and Jones (2005)

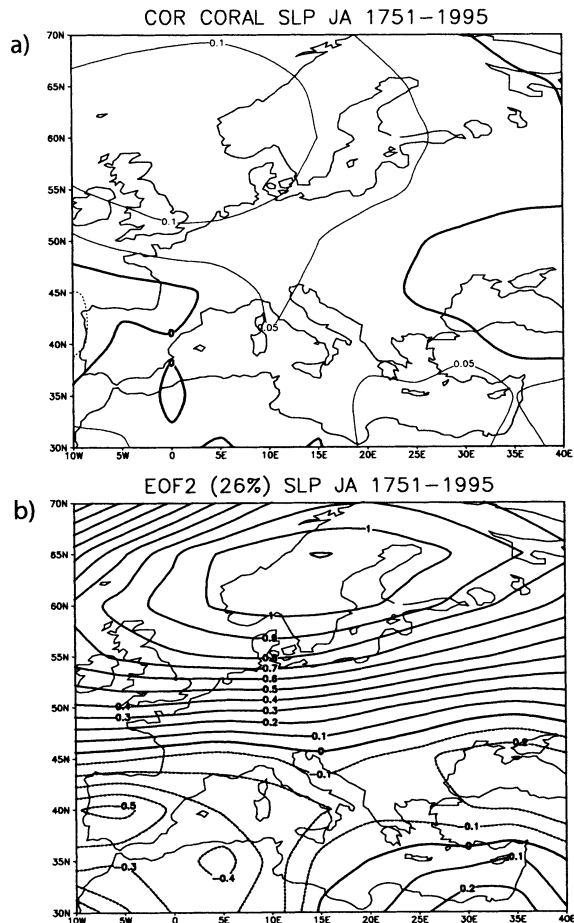


Figure 7 (a) The correlation map for the summer coral $\delta^{18}\text{O}$ record and reconstructed fields of sea-level pressure (SLP) over the European-Middle East (EME) region for July–August (JA) is shown. (b) The corresponding second Empirical Orthogonal Function (EOF) of reconstructed SLP over the EME region for JA is also shown. The variance explained by the EOF is indicated. Prior to the analyses the data were detrended and normalized. The period is AD 1751–1995. Reconstructed SLP data are from Luterbacher *et al.* (2002)

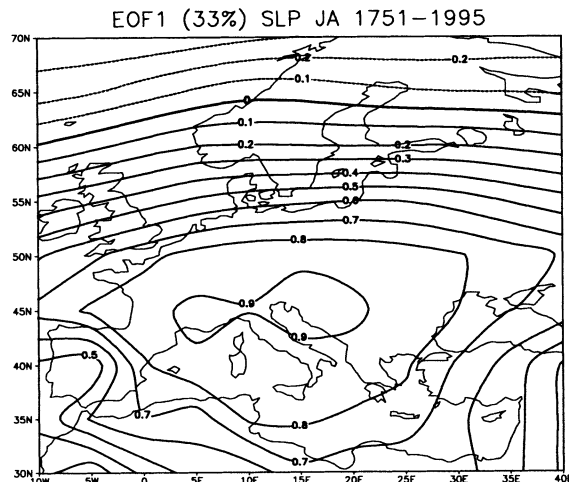


Figure 8 The first Empirical Orthogonal Function (EOF) of reconstructed sea-level pressure (SLP) over the European-Middle East region for July–August (JA) is shown. The variance explained by the EOF is indicated. Prior to the analysis the data were detrended and normalized. The period is AD 1751–1995. Reconstructed SLP data are from Luterbacher *et al.* (2002)

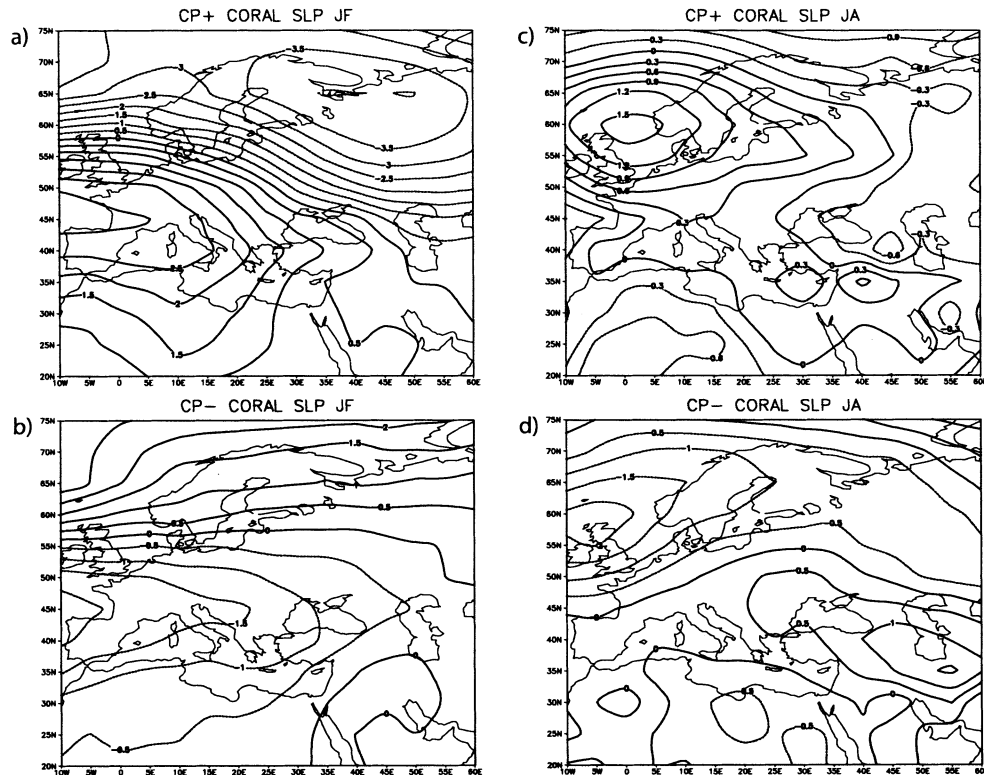


Figure 9 Sea-level pressure (SLP) anomaly patterns associated with (a) extreme positive and (b) extreme negative values in the winter coral $\delta^{18}\text{O}$ record (January–February, JF). SLP anomaly patterns associated with (c) extreme positive and (d) extreme negative values in the summer coral $\delta^{18}\text{O}$ record (July–August, JA). The threshold for extreme values is $+0.75/-0.75$ standard deviations. The period is AD 1901–1995. SLP data are from Trenberth and Paolino (1980)

are associated with positive (negative) temperature anomalies over the central and eastern (western) Mediterranean region (Xoplaki *et al.*, 2003).

Significant correlations between the summer coral $\delta^{18}\text{O}$ record and temperature only occur on a regional scale, along the western margin of the northern Red Sea and large parts of northeastern Africa during the period 1901–1995 (Figure 6b). This finding is consistent with significant correlations between coral $\delta^{18}\text{O}$ and gridded SST in the northern Red Sea reported earlier (Felis *et al.*, 2000; Rimbu *et al.*, 2004). No clear relationship between the summer coral $\delta^{18}\text{O}$ record and regional or large-scale precipitation is observed.

In addition, the atmospheric circulation patterns associated with extreme values of coral $\delta^{18}\text{O}$ both in the winter and in the summer record are not entirely symmetric. For the winter coral $\delta^{18}\text{O}$ record, the spatial pattern associated with extreme positive (negative) coral $\delta^{18}\text{O}$ values projects well on the high-index (low-index) NAO regime as described by Cassou *et al.* (2004). For the summer coral $\delta^{18}\text{O}$ record, the results show a high degree of variability.

The large-scale atmospheric circulation pattern over the EME region associated with the summer coral $\delta^{18}\text{O}$ record is less well developed and less stable than that associated with the winter coral $\delta^{18}\text{O}$ record. During winter, eastern Mediterranean/Middle East climate, as reflected in the coral $\delta^{18}\text{O}$ record from the northern Red Sea, is strongly controlled by the AO/NAO phenomenon. In contrast, during summer large-scale atmospheric circulation processes are less important for northern Red Sea climate variability, albeit a connection to an atmospheric anomaly pattern with the main centre of action over southwestern Scandinavia/northern Great Britain is observed.

Conclusions

This study shows that seasonally resolved coral $\delta^{18}\text{O}$ records from the northern Red Sea provide information on regional climate variability in the eastern Mediterranean/Middle East, as well as on large-scale climate variability over the European-Middle East region for both the winter and the summer season. The association between the Ras Umm Sidd coral $\delta^{18}\text{O}$ record and the dominant mode of atmospheric variability over the European-Middle East region during winter (Arctic Oscillation/North Atlantic Oscillation) and during summer was stable over the past 250 years.

In addition, this study shows that such coral records could be used to obtain information about the frequency of weather and climate regimes in the North Atlantic realm during the pre-instrumental period, in order to put the variability of these regimes as derived from observational data (eg, Cassou *et al.*, 2004) into a long-term context.

The results suggest that seasonally resolved proxy records derived from fossil corals of the northern Red Sea have a great potential to provide information on winter and summer climate patterns in the Middle East-European region for time intervals of the Holocene epoch and the last interglacial period (eg, Felis *et al.*, 2004).

Acknowledgements

We thank two anonymous reviewers for constructive comments that significantly improved the manuscript, and the Climate Research Unit (University of East Anglia) for providing the CRU TS 2.1 data set through David Viner. This work was funded by the Bundesministerium für Bildung und Forschung

as part of KIHZ and DEKLIM, by the Helmholtz-Gemeinschaft as part of MARCOPOLI (MAR2), and by the Deutsche Forschungsgemeinschaft as part of the DFG-Research Center 'Ocean Margins' of the University of Bremen. Contribution no. RCOM0344.

References

- Cassou, C., Terray, L., Hurrell, J.W. and Deser, C. 2004: North Atlantic winter climate regimes: spatial asymmetry, stationarity with time, and oceanic forcing. *Journal of Climate* 17, 1055–68.
- Cook, E.R., D'Arrigo, R.D. and Mann, M.E. 2002: A well-verified, multiproxy reconstruction of the winter North Atlantic Oscillation Index since A.D. 1400. *Journal of Climate* 15, 1754–64.
- Eshel, G., Schrag, D.P. and Farrell, B.F. 2000: Troposphere–planetary boundary layer interaction and the evolution of ocean surface density: lessons from Red Sea corals. *Journal of Climate* 13, 339–51.
- Felis, T. and Pätzold, J. 2004: Climate reconstructions from annually banded corals. In Shiyomi, M., Kawahata, H., Koizumi, H., Tsuda, A. and Awaya, Y., editors, *Global environmental change in the ocean and on land*. Terrapub, 205–27.
- Felis, T., Pätzold, J., Loya, Y. and Wefer, G. 1998: Vertical water mass mixing and plankton blooms recorded in skeletal stable carbon isotopes of a Red Sea coral. *Journal of Geophysical Research* 103, 30731–39.
- Felis, T., Pätzold, J., Loya, Y., Fine, M., Nawar, A.H. and Wefer, G. 2000: A coral oxygen isotope record from the northern Red Sea documenting NAO, ENSO, and North Pacific teleconnections on Middle East climate variability since the year 1750. *Paleoceanography* 15, 679–94.
- Felis, T., Pätzold, J. and Loya, Y. 2003: Mean oxygen-isotope signatures in *Porites* spp. corals: inter-colony variability and correction for extension-rate effects. *Coral Reefs* 22, 328–36.
- Felis, T., Lohmann, G., Kuhnert, H., Lorenz, S.J., Scholz, D., Pätzold, J., Al-Rousan, S.A. and Al-Moghrabi, S.M. 2004: Increased seasonality in Middle East temperatures during the last interglacial period. *Nature* 429, 164–68.
- Greatbatch, R.J., Lu, J. and Peterson, K.A. 2004: Nonstationary impact of ENSO on Euro-Atlantic winter climate. *Geophysical Research Letters* 31, L022081787, doi:10.1029/2003GL018542.
- Hall, A., Clement, A., Thompson, D.W.J., Broccoli, A. and Jackson, C. 2005: The importance of atmospheric dynamics in the Northern Hemisphere wintertime climate response to changes in the Earth's orbit. *Journal of Climate* 18, 1315–25.
- Hurrell, J.W., Kushnir, Y., Visbeck, M. and Ottersen, G. 2003: An overview of the North Atlantic Oscillation. In Hurrell, J.W., Kushnir, Y., Ottersen, G. and Visbeck, M., editors, *The North Atlantic Oscillation: climate significance and environmental impact*. Geophysical Monograph Series 134, 1–35.
- Jones, P.D., Jönsson, T. and Wheeler, D. 1997: Extension to the North Atlantic Oscillation using early instrumental pressure observations from Gibraltar and South-West Iceland. *International Journal of Climatology* 17, 1433–50.
- Kondrashov, D., Feliks, Y. and Ghil, M. 2005: Oscillatory modes of extended Nile River records (A.D. 622–1922). *Geophysical Research Letters* 32, L10702, doi:10.1029/2004GL022156.
- Luterbacher, J., Xoplaki, E., Dietrich, D., Rickli, R., Jacobeit, J., Beck, C., Gyalistras, D., Schmutz, C. and Wanner, H. 2002: Reconstruction of sea level pressure fields over the eastern North Atlantic and Europe back to 1500. *Climate Dynamics* 18, 545–61.
- Luterbacher, J., Xoplaki, E., Casty, C., Wanner, H., Pauling, A., Küttel, M., Rutishauser, T., Brönnimann, S., Fischer, E., Fleitmann, D., Gonzalez-Rouco, F.J., Garcia-Herrera, R., Barriendos, M., Rodrigo, F., Gonzalez-Hidalgo, J.C., Saz, M.A., Gimeno, L., Ribera, P., Brunet, M., Paeth, H., Rimbu, N., Felis, T., Jacobeit, J., Dünkeloh, A., Zorita, E., Guiot, J., Türke, M., Alcoforado, M.J., Trigo, R., Wheeler, D., Tett, S., Mann, M.E., Touchan, R., Shindell, D.T., Silenzi, S., Montagna, P., Camuffo, D., Mariotti, A., Nanni, T., Brunetti, M., Maugeri, M., Zerefos, C., De Zolt, S., Lionello, P., Rath, V., Beltrami, H., Garnier, R. and Le Roy Ladurie, E. 2006: Mediterranean climate variability over the last centuries: a review. In Lionello, P., Nunes, M.F., Malanotte-Rizzoli, P. and Boscolo, R., editors, *The Mediterranean climate: an overview of the main characteristics and issues*. Elsevier, 27–148.
- Mitchell, T.D. and Jones, P.D. 2005: An improved method of constructing a database of monthly climate observations and associated high-resolution grids. *International Journal of Climatology* 25, 693–712.
- Pauling, A., Luterbacher, J. and Wanner, H. 2003: Evaluation of proxies for European and North Atlantic temperature field reconstructions. *Geophysical Research Letters* 30, 1787, doi:10.1029/2003GL017589.
- Paz, S., Tourre, Y.M. and Planton, S. 2003: North Africa–West Asia (NAWA) sea-level pressure patterns and its linkages with the eastern Mediterranean (EM) climate. *Geophysical Research Letters* 30, 1999, doi:10.1029/2003GL017862.
- Rimbu, N., Lohmann, G., Felis, T. and Pätzold, J. 2001: Arctic Oscillation signature in a Red Sea coral. *Geophysical Research Letters* 28, 2959–62.
- 2003: Shift in ENSO teleconnections recorded by a northern Red Sea coral. *Journal of Climate* 16, 1414–22.
- 2004: Detection of climate modes as recorded in a seasonal-resolution coral record covering the last 250 years. In Fischer, H., Kumke, T., Lohmann, G., Flöser, G., Miller, H., v. Storch, H. and Negendank, J.F.W., editors, *The climate in historical times: toward a synthesis of Holocene proxy data and climate models*. Springer-Verlag, 281–92.
- Tourre, Y.M. and Paz, S. 2004: The North-Africa/Western Asia (NAWA) sea level pressure index: a Mediterranean signature of the Northern Annular Mode (NAM). *Geophysical Research Letters* 31, L17209, doi:10.1029/2004GL020414.
- Trenberth, K.E. and Paolino, D.A. 1980: The northern hemisphere sea level pressure dataset: trends, errors and discontinuities. *Monthly Weather Review* 108, 855–72.
- Vinther, B.M., Andersen, K.K., Hansen, A.W., Schmith, T. and Jones, P.D. 2003a: Improving the Gibraltar/Reykjavik NAO index. *Geophysical Research Letters* 30, 2222, doi:10.1029/2003GL018220.
- Vinther, B.M., Johnsen, S.J., Andersen, K.K., Clausen, H.B. and Hansen, A.W. 2003b: NAO signal recorded in the stable isotopes of Greenland ice cores. *Geophysical Research Letters* 30, 1387, doi:10.1029/2002GL016193.
- von Storch, H. and Zwiers, F.W. 1999: *Statistical analysis in climate research*. Cambridge University Press.
- Xoplaki, E., Gonzalez-Rouco, F.J., Luterbacher, J. and Wanner, H. 2003: Mediterranean summer air temperature variability and its connection to the large-scale atmospheric circulation and SSTs. *Climate Dynamics* 20, 723–739.